

where

$$A = [2\alpha\gamma\delta - \beta(\gamma^2 + \delta^2)]/\Delta^{1/2}, \quad (\text{A8})$$

$$E_1^2 = \alpha^2 - \beta^2 - \Delta^{1/2}, \quad (\text{A9})$$

$$E_2^2 = \alpha^2 - \beta^2 + \Delta^{1/2}, \quad (\text{A10})$$

$$\Delta = (\gamma^2 - \delta^2)^2 - 4\alpha\beta(\gamma^2 + \delta^2) + 4\gamma\delta(\alpha^2 + \beta^2). \quad (\text{A11})$$

Putting $f(S_h^2) = 1$, Eq. (A7) yields

$$S(S+1) - \langle (S^z)^2 \rangle = \frac{1}{2}\bar{S} \left\langle \frac{\alpha - A}{E_1} \coth\left(\frac{E_1\bar{S}}{2kT}\right) + \frac{\alpha + A}{E_2} \coth\left(\frac{E_2\bar{S}}{2kT}\right) \right\rangle_K. \quad (\text{A12})$$

Near T_N , $\langle (S^z)^2 \rangle = S(S+1)/3$, and $\bar{S} \rightarrow 0$. We write, therefore,

$$2S(S+1)/3 = kT_N \langle (\alpha - A)/E_1^2 + (\alpha + A)/E_2^2 \rangle_K, \quad (\text{A13})$$

which in terms of $\alpha, \beta, \gamma, \delta$ is

$$\frac{S(S+1)}{3kT_N} = \left\langle \frac{\alpha(\alpha^2 - \beta^2) + \beta(\gamma^2 + \delta^2) - 2\alpha\gamma\delta}{[(\alpha + \beta)^2 - (\gamma + \delta)^2][(\alpha - \beta)^2 + (\gamma - \delta)^2]} \right\rangle_K. \quad (\text{A14})$$

Using Eqs. (A3) to (A6), we have evaluated T_N by computer and the results are shown in Fig. 2.

Paramagnetic Resonance of S-State Ions in Metals of High Paramagnetic Susceptibility

D. SHALTIEL, J. H. WERNICK, AND H. J. WILLIAMS
Bell Telephone Laboratories, Murray Hill, New Jersey

AND

M. PETER

Institut de Physique Experimentale, University of Geneva, Geneva, Switzerland

(Received 19 March 1964)

The paramagnetic resonance of Gd^{3+} in metals shows g shifts with respect to the free ionic g value which are due to the valence-electron polarization in metallic hosts, and the effective exchange interaction of Gd^{3+} with these valence electrons. These shifts have been studied in metals and intermetallic compounds with high paramagnetic susceptibility such as Pd, Ni_5Y , and Pd_3U and in many alloys involving these metals and compounds. The effective exchange interaction is found to be generally much smaller than expected from the atomic spectra. It is negative for valence bands of d character and positive in valence bands of $5f$ and s character, and is therefore not the result of simple atomic exchange only. The shape of the Gd resonance lines gives information on the spatial variations in the valence-electron polarization of the host metals. Thus, it was found that Pd alloyed with La or H segregates into two phases. The valence-electron polarization can be altered by admixture of other magnetic ions, and it was therefore possible to measure the exchange interaction for many rare earths and Fe, Co, Ni in Pd, and some rare earths in Ni_5Y . The Gd line shape in these experiments allowed a study of the nonlocal character of the valence-electron susceptibility, and it appears that in Pd and in Ni_5Y this susceptibility has a larger range than predicted by the free-electron calculation of Ruderman-Kittel-Yosida.

I. INTRODUCTION

IN a previous article, we have described the electron paramagnetic resonance (EPR) of $GdAl_2$ and of dilute alloys of Gd in the Pd series.¹ The present paper is a continuation of this work. The technique previously described is exploited and expanded to study the coupling between valence electrons and magnetic ions in several classes of alloys. At the same time we studied the variation of the induced valence-electron polarization, from the macroscopic down to the atomic scale. It is found that the explanation of the valence-electron

polarization as due to direct ion-valence-electron exchange processes only² has to be abandoned. Also, it appears that the spatial variation of the valence-electron polarization is, in several cases, of a different nature than the one predicted by the theory of the susceptibility of a free-electron gas.^{3,4}

The EPR spectra observed were due to ions in the S state (Gd^{3+} , and Mn in a not quite understood valence state) and consisted of a single resonance line, of about 500 G half-half-width. The g value of this

¹ M. Peter, D. Shaltiel, J. H. Wernick, H. J. Williams, J. B. Mock, and R. C. Sherwood, *Phys. Rev.* **126**, 1395 (1962).

² C. Zener, *Phys. Rev.* **87**, 440 (1951).

³ M. A. Ruderman and C. Kittel, *Phys. Rev.* **96**, 99 (1954).

⁴ K. Yosida, *Phys. Rev.* **106**, 893 (1954).

line showed a shift which correlated with the susceptibility of the host metal, as was particularly evident in the case of the Pd-series alloys, where the susceptibility undergoes very strong variations with composition. The observations were quite consistent with the model of an effective exchange interaction between the Gd and the metallic valence electrons. The electron polarization, $\sigma(\mathbf{x})$, created by any one of the magnetic ions is the nonlocal response by the valence electrons to the perturbation created by the valence-electron-ion exchange interactions. In our study we have assumed the exchange interaction to be well localized, so that the spatial dependence of $\sigma(\mathbf{x})$ is essentially the response of the valence-electron gas to a delta function, and the strength of the effects depends only on the average of the exchange interaction. In several alloy systems, it was found that the spatial average of $\sigma(\mathbf{x})$ was such as to be consistent with a negative average exchange interaction. From this, it appeared that the basic interaction could not be, as was previously widely assumed,^{2,4} the first-order valence-electron-ion exchange interaction, only. The resonance results are based on the observation of either of two different phenomena. The first one is the direct effect mentioned before, i.e., the *shift* of the paramagnetic resonance of Gd or Mn due to the exchange field of the conduction electrons which is caused by the polarization due to the applied magnetic field.^{1,5} The second phenomenon, the indirect effect, is caused by the action of the z component of the exchange field of the conduction valence electrons which is caused by other magnetic impurity ions.⁶ These latter measurements contain information on the exchange interaction of the other magnetic impurities, and also on the shape of the magnetic response function. The shape of that response function has been well studied theoretically in the free-electron approximation and is predicted to be such that dilute magnetic impurities should produce a broadening of the Gd lines which exceeds any shift due to the indirect effect.⁴ One of the experimental results of this paper is, however, that in several cases the observed shifts exceed the observed broadenings. Simple statistical analysis makes it possible to relate these results to an anomalously long range of the valence-electron susceptibility. Besides the direct and indirect effects, we have also studied the susceptibilities in the undoped and doped alloys. Knowledge of the susceptibility is necessary for the evaluation of the exchange interaction, as an indication for the magnetic state of the impurities, and for the control of the quality of the alloys used in the experiments. In the present paper, we give first a brief analysis of the experiments. Then we report the result of EPR study of the direct and indirect effects, and of susceptibility measurements on the following systems: (A)

the rare earths in the Pd series, (B) transition-group elements in Pd, (C) the PdU system, and (D) the CaCu₅ systems with mostly Ni and Cu in the Cu site.⁷ Finally, we give a discussion.

II. ANALYSIS OF THE EPR EXPERIMENTS

In this section we consider the paramagnetic resonance signal to be expected from a system A of paramagnetic ions dissolved in a metallic host lattice. We assume that also a second species of paramagnetic ions, system B , is dissolved in the same lattice, but we are interested only in the spectrum of the A system. In our experiments, the A system consists of the Gd ions, the B system of other magnetic ions, whose relaxation times are too short to give an observable resonance spectrum. The B system is only observed through its indirect effects (shift and broadening) on the resonance of the A system.

Both the A and B systems interact through an effective exchange interaction with the valence electrons. Let $J_n(\mathbf{y}-\mathbf{R}_n)\mathbf{S}_n\sigma(\mathbf{y})d\mathbf{y}$ be the effective exchange interaction between an ion of spin \mathbf{S}_n situated at \mathbf{R}_n and the conduction-electron spin $\sigma(\mathbf{y})d\mathbf{y}$ in the volume element $d\mathbf{y}$. Then we can determine the spin density $\sigma(\mathbf{x})$ with the help of a nonlocal susceptibility function of $f(\mathbf{y}-\mathbf{x})$. This function may be normalized to $q_1 = \int_V f(\mathbf{y}-\mathbf{x})d\mathbf{y}$. q_1 is related to the susceptibility of the host lattice by $q_1 = 2\chi_0/g_e^2\beta^2$ (β is the Bohr magneton and g_e the g factor of the valence electrons). If we label the ions of system A with the index a , the ions of system B with the index b , we can write

$$\sigma(\mathbf{x}) = \frac{1}{2V} \int_V \left[g_e\beta\mathbf{H} + \sum_a J_a(\mathbf{y}-\mathbf{R}_a)\mathbf{S}_a + \sum_b J_b(\mathbf{y}-\mathbf{R}_b)\mathbf{S}_b \right] f(\mathbf{y}-\mathbf{x})d\mathbf{y}. \quad (1)$$

V is the volume of the sample, and \mathbf{H} is the external magnetic field in the z direction, of strength H_z . The energy of valence electrons and ions together is then given by the spin Hamiltonian

$$\mathcal{H} = -\frac{1}{2} \int_V \sigma(\mathbf{x}) \left[g_e\beta\mathbf{H} + \sum_a J_a(\mathbf{x}-\mathbf{R}_a)\mathbf{S}_a + \sum_b J_b(\mathbf{x}-\mathbf{R}_b)\mathbf{S}_b \right] d\mathbf{x} - \sum_a g_a\beta\mathbf{S}_a\mathbf{H} - \sum_b g_b\beta\mathbf{S}_b\mathbf{H}. \quad (2)$$

Since, in our experiments, $J_n(\mathbf{x}-\mathbf{R}_m)$ represents the effective exchange interaction with a well-localized

⁵ J. Owen, M. E. Brown, W. D. Knight, and C. Kittel, Phys. Rev. **102**, 1501 (1956).

⁶ M. Peter, D. Shaltiel, J. H. Wernick, H. J. Williams, J. B. Mock, and R. C. Sherwood, Phys. Rev. Letters **9**, 50 (1962).

⁷ A preliminary account of Gd in CaCu₅ intermetallic compounds was given at the American Physical Society Meeting, March 1962, Bull. Am. Phys. Soc. **8**, 249 (1962).

ion, we can simplify the interaction $J_n(\mathbf{x}-\mathbf{R}_n) = (V/n_0)\bar{J}_n\delta(\mathbf{x}-\mathbf{R}_n)$; (n_0/V) is the number of lattice sites per cubic centimeter.

The spin Hamiltonian now becomes

$$\begin{aligned} \mathcal{H} = & -g_a \sum_a \beta \mathbf{H} \mathbf{S}_a - g_b \sum_b \beta \mathbf{H} \mathbf{S}_b \\ & - (1/2n_0) \sum_a \bar{J}_a g_a \beta q_1 \mathbf{S}_a \mathbf{H} - (1/2n_0) \sum_b \bar{J}_b g_b \beta q_1 \mathbf{S}_b \mathbf{H} \\ & - (V/4n_0^2) \left[\sum_a \sum_{a'} \bar{J}_a^2 \mathbf{S}_a \mathbf{S}_{a'} f(\mathbf{R}_a - \mathbf{R}_{a'}) \right. \\ & \quad \left. + \sum_b \sum_{b'} \bar{J}_b^2 \mathbf{S}_b \mathbf{S}_{b'} f(\mathbf{R}_b - \mathbf{R}_{b'}) \right] \\ & - (V/4n_0^2) \sum_a \sum_b \bar{J}_a \bar{J}_b \mathbf{S}_a \mathbf{S}_b f(\mathbf{R}_a - \mathbf{R}_b). \end{aligned}$$

With this spin Hamiltonian, we must determine the resonance field H_r for the center of the EPR resonance line due to magnetic transitions of the A system. If $I(H)$ is the normalized resonance line shape, then $\int (H' - H_r) \times I(H') dH' = 0$. Furthermore, we must estimate the width DH of the resonance line, best defined through $(DH)^2 = B = \int (H' - H_r)^2 I(H') dH'$. As usual, the resonance condition will be characterized by a g value

$$g = h\nu_{\text{res}}/\beta H_r = g_a + \Delta g_0 + \Delta g_B. \quad (3)$$

g_a , the g factor of the a ions, comes from the first term in \mathcal{H} . Δg_0 comes from the third term, and Δg_B gives the influence of the B system, contained in the last term of \mathcal{H} .

The terms in $\mathbf{S}_a \mathbf{S}_a$, commute with $\sum_a \mathbf{S}_a$ and will not influence the line position.

The expectation value of $\mathbf{S}_a \mathbf{S}_b$ will be $S_{az} \langle S_{bz} \rangle$ if $g_a \neq g_b$, i.e., if the two spins precess at different rates. The spins of the b ions are coupled to the orbital momentum of the same ions by spin-orbit coupling (only the a ion will in general be in an S state). The total momentum \mathbf{J}_b will undergo fast thermal relaxation, so that the a ions will see only the thermal average of \mathbf{J}_b during a transition. Under these conditions, we have to set $\langle S_{bz} \rangle = g_b(g_b - 1) \mathbf{J}_b(\mathbf{J}_b + 1) \beta H_z / 3kT$, where g_b is the Landé g factor of the b ion and \mathbf{J}_b the quantum number of its total momentum. The energy difference ΔE_{ab} for the transition of an a ion in presence of one b ion is now

$$\begin{aligned} \Delta E_{ab} = & H_z(g_a\beta + \bar{J}_a g_a \beta q_1 / 2n_0) \\ & + V(\bar{J}_a \bar{J}_b / 2n_0^2) \langle S_{bz} \rangle f(\mathbf{R}_a - \mathbf{R}_b). \quad (4) \end{aligned}$$

The average energy difference $\Delta E = h\nu_{\text{res}}$ for the flip of an a ion is now obtained by summing Eq. (4) over all positions \mathbf{R}_b , assuming that at each site \mathbf{R}_b there sits a b ion with probability c_B , where c_B is the concentration of the b ions. The sum over the sites \mathbf{R}_b we approximate by integrating over \mathbf{R}_b and dividing by V .

From these considerations, we obtain⁸

$$\Delta g_0 = \bar{J}_a g_a q_1 / 2n_0 = \bar{J}_a \chi_0 V / g_a \beta^2 n_0, \quad (5')$$

$$\Delta g_B = \bar{J}_b (g_b - 1) \Delta g_0 \chi_B V / g_b g_b n_0 \beta^2 \alpha. \quad (5'')$$

Δg_0 is proportional to the susceptibility of the valence electrons of the host metal χ_0 and independent of the susceptibility of the A system χ_A . A discussion of this point, and an alternate derivation of Δg_0 , is given in Appendix A. Δg_B is proportional to the susceptibility of the ions in the B system, $\chi_B = g_b^2 \mathbf{J}_b(\mathbf{J}_b + 1) \beta^2 e_B n_0 / 3kTV$.

There remains the determination of the mean-square deviation B from the mean resonance field $H_r = h\nu_{\text{res}}/\beta g$. Van Vleck's moment analysis⁹ cannot be immediately applied since, in our case, the field for resonance in presence of the b ions, $H_r = h\nu_{\text{res}}/\beta g$ deviates from the field $H_c = h\nu_{\text{res}}/\beta g_0$ for resonance in absence of the B system ($g_0 = g_a + \Delta g_0$).

The situation becomes clear in the case where the concentration of the a ions c_A is small compared to c_B . Without this restriction, the situation is complicated by the exchange interaction within the A system; however, these effects are not yet important in our experiments where $c_B \sim c_A$. With our restrictions, the shape function $I(H)$ for the resonance of an a ion in presence of the B system is found from the following statistical model: If $I_0(H)$ is the normalized resonance function of the a ion in absence of the B system, centered on H_c , then a b ion at the site \mathbf{R} will shift $I_0(H)$ to $I_0(H')$ with $H' = H + h$ and $h = (\bar{J}_a \bar{J}_b / 2n_0 g_0 \beta) \times f(\mathbf{R}_a - \mathbf{R}) \langle S_{bz} \rangle$. If the b ion is distributed at random, the normalized probability for this shift to occur will be $F(h) dh = \int_{K(h)} d\mathbf{R} / V$, where $K(h)$ is the region of space where the ions produce a shift between h and dh . The line shape for one b ion distributed at random is $I_1(H) = \int_{-\infty}^{\infty} I_0(H') F(H' - H) dH'$. If we approximate $I_0(H)$ by a delta function, the moments of $I_1(H)$ will be

$$\begin{aligned} p_k = & \int_{-\infty}^{\infty} (H - H_c)^k I_1(H) dH \\ = & (-V \bar{J}_a \bar{J}_b \langle S_{bz} \rangle / 2g_0 \beta n_0^2)^k \int_V [f(x)]^k d\mathbf{x} / V. \quad (6) \end{aligned}$$

As long as c_B is small compared to unity, the line shape $I(H)$ for all b ions will now be given by a $c_B n_0$ -fold

⁸ The factor α in Eq. (5'') takes into account that in sum $\sum_b \bar{J}_a \bar{J}_b \mathbf{S}_a \mathbf{S}_b f(\mathbf{R}_a - \mathbf{R}_b)$ $\mathbf{R}_a \neq \mathbf{R}_b$. The integral in (5'') must therefore be taken with a lower cutoff; hence

$$\alpha = \int_0^{\infty} f(x) dx / \int_{|\mathbf{x}| > r_c} f(x) dx.$$

The value of α for $f_M(\mathbf{x}) \sim 1$. However, there exists now a better estimate for $f(\mathbf{x})$ [B. Giovannini, J. R. Schrieffer, and M. Peter, Phys. Rev. Letters 12, 736 (1964)]. From this estimate, it follows that $\alpha = 5$. For this reason, we give in Table II also the values of \bar{J}_{RE} for $\alpha = 5$ and plot these values in Fig. 21. The work of Giovannini *et al.* explains also the narrow linewidths discussed in IV B.

⁹ J. H. Van Vleck, Phys. Rev. 74, 1168 (1948).

convolution of $I_0(H)$ with $F(H)$. The first moment $P_1 = \int_{-\infty}^{\infty} I_0(H)(H-H_c)dH$ determines the line shift $P_1 = H_r - H_c = S$, and the second moment $P_2 = \int_{-\infty}^{\infty} I_0(H) \times (H-H_c)^2 dH$ determines the mean-square deviation B : $B = P_2 - P_1^2$. According to the theory of semi-invariants,¹⁰ we get $P_1 = n_0 c_B \phi_1$ and $B = c_B n_0 (\phi_2 - \phi_1^2) = c_B n_0 \phi_2 - (1/c_B n_0) P_1^2$. The second term for B is negligible, and hence we find that B , the mean-square deviation with respect to the center of the *shifted* line, is just given by the formula given by Van Vleck for the case of negligible shifts: $B = c_B n_0 \phi_2$.

In calculating ϕ_2 , we have taken $\langle S_{zb} \rangle^2$, whereas Van Vleck took $\langle S_{zb}^2 \rangle$. We made the former choice since, as stated above, in our experiments the b ions undergo thermal relaxation which is fast compared to the radiation time of the a ions. For later reference, we can now easily calculate B and S for three specific functions $f(\mathbf{x})$. These three functions depend only on the radial coordinate $x = |\mathbf{x}|$ and are normalized to the density of states at the Fermi surface, which has the value $\eta(E_f) = 2\chi_0 / (g_s \beta)^2$ in the free-electron case. With this normalization, the shift S is already determined. We obtain $S = -H_r \Delta g_B / g_0 = -c_B n_0 q_1 \int_a \int_b \langle S_{bz} \rangle / 2g_0 \beta n_0^2$. Instead of giving B , we determine next the parameter $R = S^2 / B$, which is easily related to the experimental data. It is independent of normalization, and measures the square of the shift induced by the B system, divided by the broadening due to the B system.

Our three specific functions are:

(1) The Rudermann-Kittel³ function f_K which is the susceptibility of the free-electron gas, calculated neglecting correlation and exchange:

$$f_K(\mathbf{x}) = [(3n)^2 \pi / 2VE_f] (\sin 2k_f x - 2k_f x \cos 2k_f x) / (2k_f x)^4.$$

Here, $n = V k_f^3 / 3\pi^2$ is the number of valence electrons in Fermi sphere.

(2) A function discussed by Yosida, $f_Y(\mathbf{x})$ [Ref. 4, Eq. (2.24)]. This function has a simple Fourier transform: $f_Y(q) = 2$ for $0 \leq q \leq 2k_f$ and f_Y zero otherwise. This leads to

$$f_Y(\mathbf{x}) = [(3n)^2 / VE_f] (\sin 2k_f x - 2k_f x \cos 2k_f x) / (2k_f x)^3.$$

(3) A model function $f_M(\mathbf{x})$ with a simple appearance in space, which is defined by $f_M(\mathbf{x}) = 3\eta(E_f) / 4\pi r_0^3$ for $0 < |\mathbf{x}| < r_0$, $f_M(\mathbf{x}) = 0$ otherwise.⁶ For these three functions we find the following values for the parameter R : $R_K = 5c_B n_0 / 2n\pi^2$; $R_Y = c_B n_0 / 4n$; $R_M = 4\pi r_0^3 c_B n_0 / 3V$. R_K and R_Y are easily estimated for typical experimental conditions such as $c_B = 2 \times 10^{-2}$, $n_0 = 6 \times 10^{22}$, $n = 3.6 \times 10^{22}$. We obtain $R_K \sim R_Y = 8.3 \times 10^{-8}$. R_M turns out to have a simple meaning: It represents the number of b ions in a sphere of radius r_0 . We get for R_M the value R_Y in the above example, if we choose for the radius the value $r_0 = 1.2 \text{ \AA}$. r_0 determined in this way represents the effective range of the susceptibility function.

¹⁰ W. R. Bennet, Proc. Inst. Radio Engrs. 44, 609 (1956).

Susceptibility Measurements

The susceptibility measurements on the dilute rare-earth alloys were analyzed by decomposing the susceptibility χ into two parts, the ionic susceptibility χ_{ion} , and the unperturbed host susceptibility χ_0 :

$$\chi = \chi_{\text{ion}} + \chi_0.$$

χ_0 depends, in general, on T .

The temperature dependence of χ_{ion} is given, in the limit of small ion-valence-electron interaction, by a Curie-Weiss law,

$$\chi_{\text{ion}} = m\beta^2 J(J+1)g_{\text{ion}}^2 / 3Vk(T-T_0) = mP^2 / 3Vk(T-T_0)$$

(m/V is the number of ions per cubic centimeter).

This separation of χ into two parts was found to work satisfactorily in the case of the rare earths (see below). However, in cases such as that of the transition metals in Pd, the ion-electron interaction is sufficiently strong to make this decomposition an insufficient approximation. Clogston¹¹ has found that χ_{ion} can be made to show Curie-Weiss behavior if the effective moment P is set proportional to χ_0 .

We have slightly generalized this dependence by assuming that the magnetic moment associated with the magnetic impurity is a linear function of the susceptibility of the undoped Pd.

$$P(T) = P_0 [1 + \alpha \chi_0(T)], \quad (7)$$

where P_0 is the unenhanced magnetic moment and α is the enhancement factor. For $\alpha \chi_0 \gg 1$ this leads to Clogston *et al.*'s assumption.

III. EXPERIMENTAL RESULTS

A. Rare Earth in Pd

a. Susceptibility Measurements

We have measured the susceptibility of dilute rare-earth alloys in Pd for most of the rare earths. X-ray measurements have shown an increase of the lattice constant with the addition of rare earth indicating that the rare earths (RE) go into solid solution with the Pd for low impurity concentrations. In Figs. 1 and 2 are plotted the observed values of $1/(\chi - \chi_0)$ for some of the rare-earth Pd. The function $1/(\chi - \chi_0)$ is seen to be a linear function of the temperature (χ is the total measured susceptibility, χ_0 is the background susceptibility). χ_0 was found by measuring the susceptibility of Pd alloys where Lu replaced the rare earths. Lu rather than La was used as reference since we found that La does not go into solid solutions, but forms an additional phase, while Lu is soluble in Pd. This result was established from the following observations:

(1) The Lu susceptibility falls into the normalized curve of the susceptibility of Pd alloys at a given

¹¹ A. M. Clogston, B. T. Matthias, M. Peter, H. J. Williams, E. Corenzwit, and R. C. Sherwood, Phys. Rev. 125, 541 (1962).

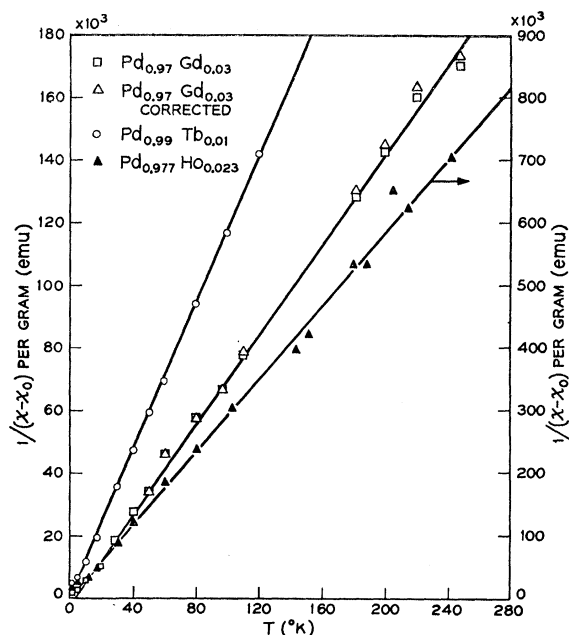


FIG. 1. $1/(\chi-\chi_0)$ curves of small concentrations of Gd, Tb, and Ho in Pd. For Gd we give also the corrected points due to the interaction with conduction electrons. Note the small difference between the two.

temperature as a function of the ratio between the number of conduction electrons added to the valence band in alloying the total number of atoms¹² (Lu gives three electrons per atom). The La susceptibility does not fit into this curve.

(2) X-ray measurements show an increase in the lattice constant for Lu but not for La where only broadening of the x-ray lines is observed.

(3) As discussed later, the addition of Lu does not shift the EPR line of Gd, while the addition of La produces an additional line indicating the existence of a second phase.

Since the background susceptibility around room temperature was from 40 to 90% of the total susceptibility, we expect large errors in the calculated values at this temperature region, and therefore less weight was given to these values when plotting the susceptibility curves.

Table I gives the effective magnetic moment of some of the rare earths in Pd as derived from the slope of the curves in Figs. 1 and 2. The concentrations given are the ones of the constituents before alloying, and deviations of 10% are possible. In the case of Ho, the concentration was analyzed and found to agree with the nominal value. The moments are in most cases close to the free ionic values. However, the susceptibility of 4% Ce in Pd is lower than our standard background susceptibility down to 100°K (Fig. 3). The effective

¹² L. F. Bates and S. J. Leach, Proc. Phys. Soc. (London) **69**, 997 (1956).

TABLE I. μ_{eff} of R.E. elements in Pd.

Rare earth	Concentration atom %	μ_{eff}	θ °K
Ce	4.0	1.1	4
Pr	2	3.3	-4
Nd	3.2	3.07	-2
Gd	3	6.28	+3
Tb	1.0	8.4	0
Ho	0.23	10.8	0
Yb	4.0	4.54	-2

magnetic moment derived from measurements at temperatures below 100°K is 1.1 Bohr, lower than the free-ion value of 2.4 Bohr magnetons.

The interaction of the conduction electrons with the local magnetic moments lead to the correction of the susceptibility curves discussed above. The corrected $1/(\chi-\chi_0)$ values for Gd in Pd are shown in Fig. 1 together with the uncorrected ones. We see that the difference between them is small and therefore we did not apply the corrections.

b. EPR

The paramagnetic resonance of Gd in Pd has been described in our earlier paper,¹ and the experimental details of the resonance measurements on ions in metallic solution are given there. A partial account of the measurements on Gd, Pd alloys, in which other magnetic ions are also dissolved, was given in Ref. 6.

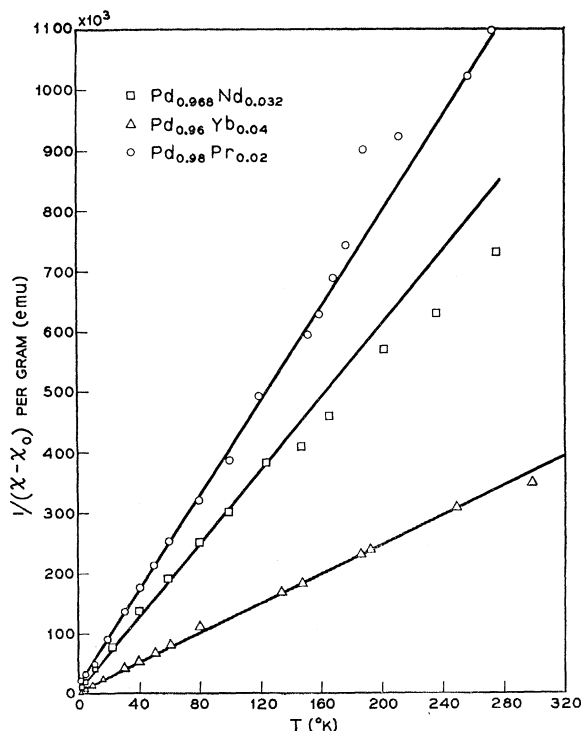


FIG. 2. $1/(\chi-\chi_0)$ of Nd, Pr, and Yb in Pd.

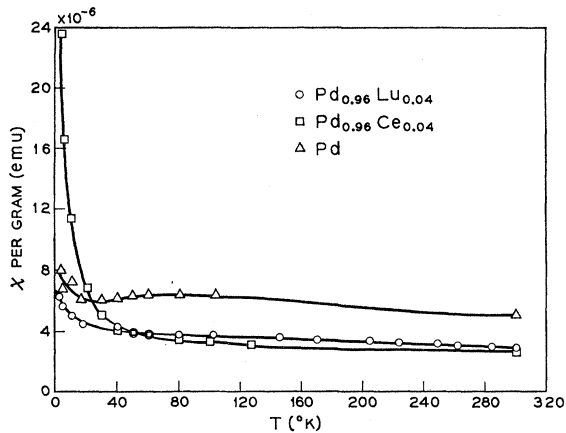


FIG. 3. Total susceptibility of Pd and of 4% Lu and Ce in Pd. The slight increase of the susceptibility in Pd at low temperature is due to impurities.

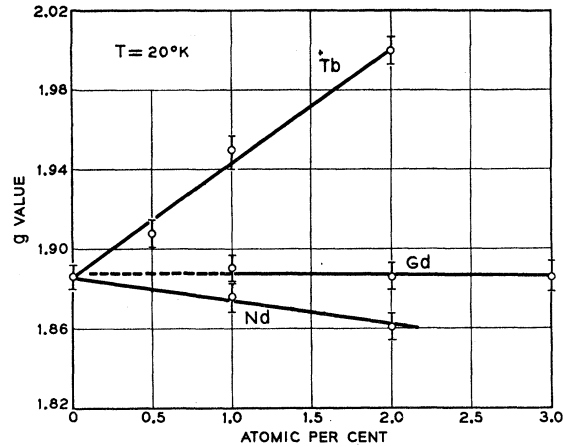


FIG. 5. *g* value of 2 at. % Gd in Pd as a function of the Tb and Nd concentration.

This section reports the resonance results obtained for Gd in Pd in presence of dilute solution of most of the rare-earth ions.

Figure 4 shows the *g* value of Gd in Pd, with 2% RE plotted against the positions of the RE in the periodic system. For Gd alone we observe a negative shift and therefore its exchange constant is negative. Except for Ce, Eu, Sm, and Yb, which will be discussed separately, the additional *g* shifts are of opposite sign for the RE to the left and to the right of Gd. Figure 5 shows that the *Gd/g* value in Pd at 20°K varies linearly with the Tb or Nd concentration, and that it is independent of the Gd concentration. Figure 6 shows the temperature dependence of the Gd *g* value in Pd for an undoped sample and for a sample doped with Tb, Pr, and Sm. Figure 7 shows that the changes of the *g* value in the Tb- and Pr-doped alloys shown in Fig. 6 are a linear function of the part of the susceptibility of these alloys which is due to the *B* atoms. The Gd, Pd sample of Fig. 6 was used for the determination of the axis $\Delta g_B = 0$.

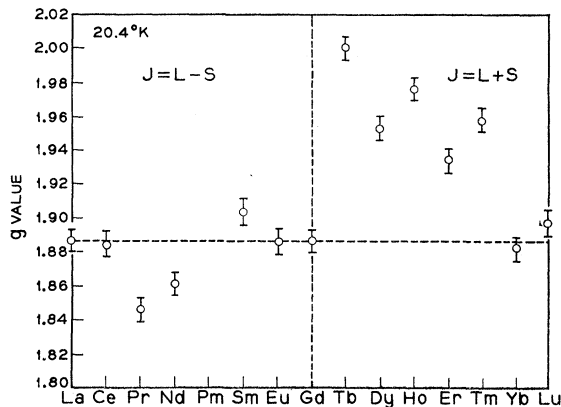


FIG. 4. *g* value of Gd in alloys of 96 at. % Pd, 2 at. % Gd, and 2 at. % RE.

These results can be interpreted with the help of Eq. (5). The values for the exchange interaction deduced from this equation, and using the *g* shifts measured at 20°K are given in Table II. χ_A and χ_B were either derived from the measured susceptibilities shown in Figs. 1 and 2 or calculated using the magnetic

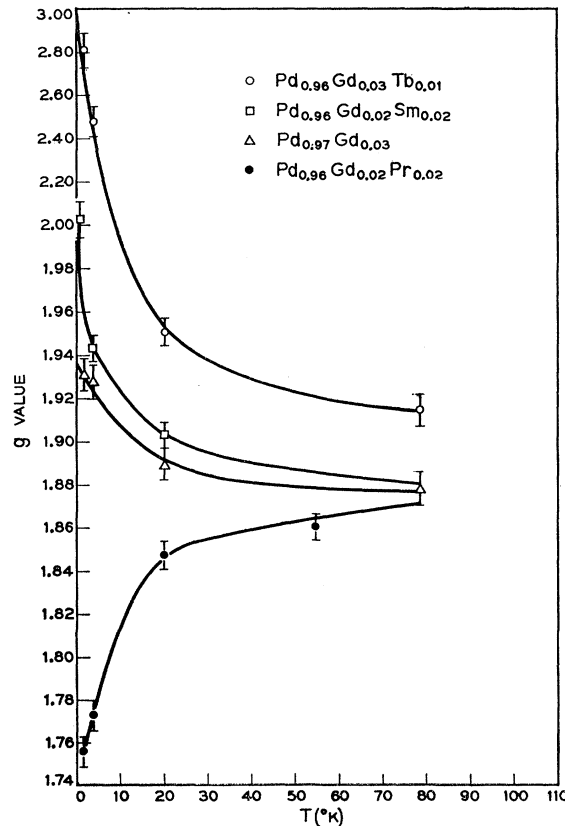


FIG. 6. *g* value of Gd in the alloys $\text{Pd}_{0.96}\text{Tb}_{0.01}\text{Gd}_{0.03}$; $\text{Pd}_{0.96}\text{Sm}_{0.02}\text{Gd}_{0.02}$; $\text{Pd}_{0.97}\text{Gd}_{0.03}$; $\text{Pd}_{0.96}\text{Gd}_{0.02}\text{Pr}_{0.02}$; as a function of temperature.

TABLE II. Gd linewidth and the shift in line position S for various RE elements in Pd_{0.96}, Gd_{0.02}, RE_{0.02} alloys at 20.4°K, and exchange interaction J_{RE} for various RE in Pd.

Rare earth	$DH_{RE} \pm 10\%$	$S = H_{RE} - H_{Gd}$	$\Delta DH = (DH_{RE}^2 - DH_{Gd}^2)^{1/2}$	$S/\Delta DH$	\bar{J}_{RE}^b eV	$\bar{J}_{RE}^c (\alpha=5)$ eV
Ce	650					
Pr	620	+ 425	~0	>>1	-0.066	-0.33
Nd	840	+ 260	470	0.55	-0.028	-0.14
Sm	900	- 120	760	0.16	^a	
Eu	610				0	
Gd	675				-0.009	-0.009
Tb	1230	-1000	1020	0.98	-0.018	-0.09
Dy	840	- 200	495	0.40	-0.012	-0.06
Ho	850	- 800	502	1.6	-0.019	-0.09
Er	790	- 250	476	0.52	-0.013	-0.06
Tm	735	- 640	270	2.3	-0.043	-0.21
Yb ^a					^a	
Lu	520				0	

^a See text.

^b The values here differ from those given in Ref. 6 due to an error in the formula for λ_{RE} which should be read $\lambda_{RE} = J_{RE}(g_{RE} - 1)/2n_0\beta^2 g_{RE}$.

^c See Ref. 8.

moments of the free ions and assuming a Curie law with zero Curie temperature. The errors introduced by this latter assumption are small (see Table I).

Both \bar{J}_a and \bar{J}_b are found to be negative in Pd. Hence

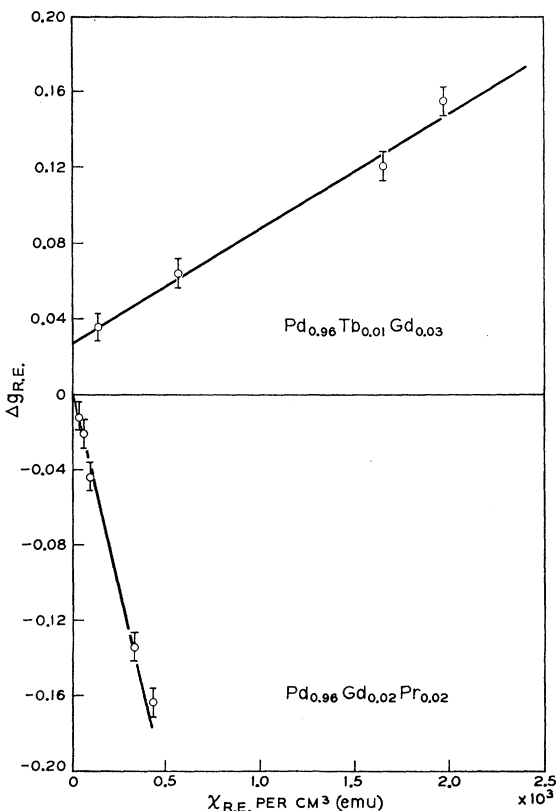


FIG. 7. The change of the g value, Δg_{RE} , in the alloys Pd_{0.96}Gd_{0.02}Tb_{0.01} and Pd_{0.96}Pr_{0.02}Gd_{0.02} as function of volume susceptibilities χ_{Tb} and χ_{Pr} , respectively. Δg_{RE} and χ are parametric functions of the temperature. The susceptibilities were measured in 1% Tb, 99% Pd, and 2% Pr, 98% Pd and the Pd susceptibility subtracted. The g value of the undoped samples of Gd in Pd was used to establish the axis $\Delta g_{RE}=0$.

the conduction-electron polarization is decreased by the RE that are situated to the right of Gd in the periodic system, $\langle(\mathbf{S} \cdot \mathbf{J})\rangle > 0$. This decrease results in less negative g shifts of the Gd ions, i.e., g_{eff} is increased. In the case of the Tb-doped sample shown in Fig. 6, there occurred even a reversal of the sign of the conduction electron polarization, since at 4.2°K and at 1.2°K values larger than the free ionic value are observed. For Nd and Pr the spins are antiparallel to the total angular momentum \mathbf{J} ; therefore, their interaction with the conduction electrons will increase the conduction electron polarization and shift the g value of Gd to lower values.

No additional g shifts were observed for Ce even at 4.2°K. The susceptibility measurements discussed above have shown that the Ce magnetic moment is much lower than the moment of free Ce³⁺ indicating that the Ce is not in a pure trivalent state even at low temperatures. It is possible that part of the Ce is in a quadrivalent state as we found that Ce in intermetallic compounds with the Pt group elements like CeRh₂ and CePr₂ is in the quadrivalent state.¹³

Sm produces a positive g shift opposite to what one expects from the simple model. White and Van Vleck¹⁴ have pointed out that the temperature-independent part of the susceptibility should produce an additional positive g shift, it fails to explain its temperature behavior: The Gd g value does not increase with increasing temperature as we would expect because of the temperature-dependent part of the Sm susceptibility (Fig. 6). Further investigation of this problem is important as it may provide a better understanding of the crystal-field splitting of the Sm ground state. Eu³⁺ in its ground state is nonmagnetic, and therefore no additional shift

¹³ R. M. Bozorth, B. T. Matthias, H. Suhl, E. Corenzwit, and D. D. Davis, Phys. Rev. **115**, 1595 (1959).

¹⁴ J. White and J. H. Van Vleck, Phys. Rev. Letters **6**, 412 (1963).

is expected, in agreement with our experimental results.

The Yb experiments gave different results in three different samples. It seems that the g value decreases when Yb is added to Gd, opposite to what we observed for the other rare earths to the right of Gd. Further work is being done on this element to clarify the problem.

La and Lu have empty and full f shells, respectively, and therefore they do not produce any shift. However, in La an additional line was observed with $g=2.00$. The ratio of the intensities of the two lines was roughly proportional to the La concentration. These results indicate that two phases are present in these alloys. La³⁺ has the largest radius in the RE ions,¹⁵ and probably even small amounts of La do not go into solid solution with Pd. Hydrogen in Pd has shown similar effects on the Gd resonance, and there also it was concluded that this is due to two phases.¹⁶

In Table II we compare the shift of the line in gauss produced by 2% RE and 2% Gd in Pd with the corresponding additional width calculated from $\Delta DH = (DH_{RE}^2 - DH_{Gd}^2)^{1/2}$, where DH_{RE} and DH_{Gd} are the linewidths of the RE-doped and the undoped samples, respectively. ΔDH represents approximately the contribution to the rms broadening due to the RE ions. In particular, this is true if both the line shape of the Gd line in absence of the RE ions, and the line shape due to the RE ions alone are Gaussian. Hence we set $(\Delta DH)^2 = B$, where B is defined in Sec. II.

The ratio of shift to width is also given in Table II. The observed values of ΔDH are much smaller than the ones predicted in Sec. II for free electrons. As will be discussed below, this is a clear indication that the simple free-electron polarization calculated to second order fails to give an adequate description of the magnetic phenomena in Pd.

B. Iron-Group Elements in Pd

a. Susceptibility

High magnetic moments (~ 10 Bohr magneton per atom) were observed for dilute Fe and Co alloys in Pd.^{11,17} Neutron¹⁸ and Mössbauer¹⁹ measurements have shown that part of the moment is on the neighboring Pd atoms. The Curie temperature of these dilute alloys are high: $60 \div 80^\circ\text{K}/\text{mole } \%$. Detailed measurements of the susceptibility of dilute iron-group elements in Pd were carried out by Gerstenberg²⁰ for the temperature range of $80^\circ\text{K} \div 1100^\circ\text{K}$. The susceptibilities are found

to deviate from the Curie-Weiss law: $\chi = m\beta^2 J(J+1) \times g_{\text{ion}}^2 / 3Vk(T-T_0)$. The deviation is more pronounced in the low-temperature range. The number of Bohr magnetons derived from the slope of the $1/\chi$ curves at low temperature is larger than at high temperature. The Curie temperatures derived from high-temperature extrapolation were much higher than those obtained from low-temperature extrapolation. Clogston *et al.*¹¹ have assumed that, at low concentrations, the local magnetic moment associated with each iron atom is proportional to the susceptibility χ_0 of the Pd. In this way they were able to obtain straight $1/(\chi-\chi_0)$ curves for a large temperature range.

We have extended Gerstenberg's measurements of the susceptibility of dilute alloys of Ni, Co, Fe, and Mn in Pd down to 1.4°K . The dashed lines in Figs. 8 and 9 give the $1/(\chi-\chi_0)$ curves of the Fe and Co alloys (χ_0 is the matrix susceptibility). Marked deviations from a Curie-Weiss law occur, particularly at low temperature. The corrected curves due to enhancement of the magnetic moment by the susceptibility of the host metal, as explained above [Eq. (7)], are shown in the same figures. These curves have a Curie-Weiss

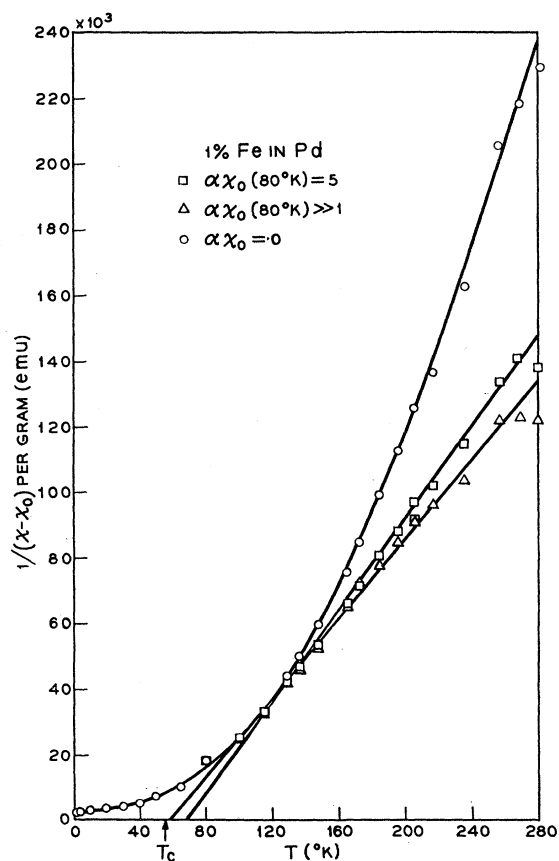


FIG. 8. The $1/(\chi-\chi_0)$ curves of 1% Fe in Pd for different enhancement factors; the number of Bohr magnetons for $\alpha\chi_0(80^\circ\text{K})=5$ and $\alpha\chi_0(80^\circ\text{K})\gg 1$ are 11.6 and 11.7, respectively; T_c was obtained from a plot of H/σ versus σ^2 (Ref. 21).

¹⁵ A. Taylor, *X-Ray Metallography* (John Wiley and Sons, Inc., New York, 1961).

¹⁶ D. Shaltiel, *J. Appl. Phys.* **84**, 1190 (1963).

¹⁷ R. M. Bozorth, D. D. Davis, and J. H. Wernick, *Proc. Phys. Soc. Japan* **17**, Suppl. B-I 112 (1962).

¹⁸ J. W. Cable, E. O. Wollan, and W. C. Koehler, *J. Appl. Phys.* **34**, 1189 (1963).

¹⁹ P. P. Craig, D. E. Nagle, W. A. Stugert, and R. D. Taylor, *Phys. Rev. Letters* **9**, 12 (1962).

²⁰ D. Gerstenberg, *Ann. Phys. (Paris)* **2**, 236 (1958).

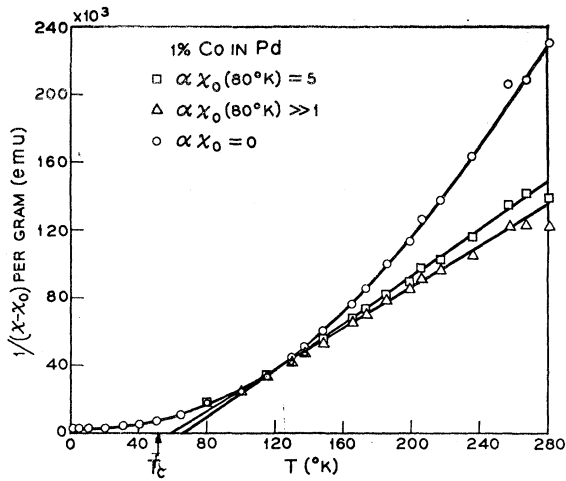


FIG. 9. $1/(\chi-\chi_0)$ curves of 1% Co in Pd for different enhancement factors; the number of Bohr magnetons for $\alpha\chi_0(80^\circ\text{K})=5$ and $\alpha\chi_0(80^\circ\text{K})$ is 9.85 and 10.5, respectively; T_c was obtained from a plot of H/σ versus σ^2 (Ref. 21).

behavior in a much larger temperature range and a more realistic value for the Curie temperature θ derived from their intersection with temperature axis than those obtained from high-temperature extrapolation.²⁰ However, it is difficult to determine by this method the enhancement factor with good accuracy for large values of $\alpha\chi_0$. This is illustrated in Figs. 8 and 9 where $1/(\chi-\chi_0)$ is plotted for $\alpha\chi_0(80^\circ\text{K})=5$ and for $\alpha\chi_0(80^\circ\text{K}) \gg 1$. In both cases, a Curie-law behavior is obtained with similar scattering of the measured points. The difference between the slopes is small. More accurate measurements at higher temperatures could give better values for the enhancement factors.

Figure 10 gives the temperature dependence of the susceptibility for concentrations up to 3.5% Ni in

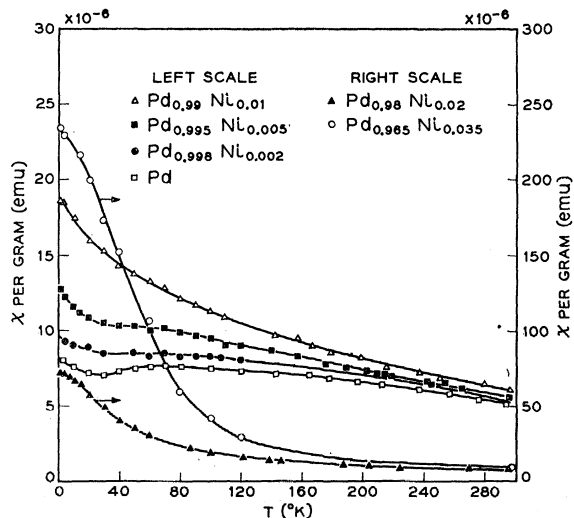


FIG. 10. Susceptibility of Pd-rich Ni alloys as a function of the temperature for various Ni concentrations.

Pd, and for temperatures between 1.4° to 300°K. The small rise in the susceptibilities for pure Pd and 0.2% Ni at low temperatures are due to small impurities present in the Pd. A relatively small increase of the susceptibility is observed for 0.2% and 0.5% Ni. The change in the susceptibility does not follow a $1/T$ law; apparently, the Ni simply increases further the high Pauli susceptibility of Pd at these low concentrations.

Further increase of the Ni concentration results in further enhancement of the magnetic susceptibility which eventually leads to the appearance of a Curie-Weiss behavior at concentrations larger than 2%. At 3.5 at. % Ni the Curie temperature derived from the

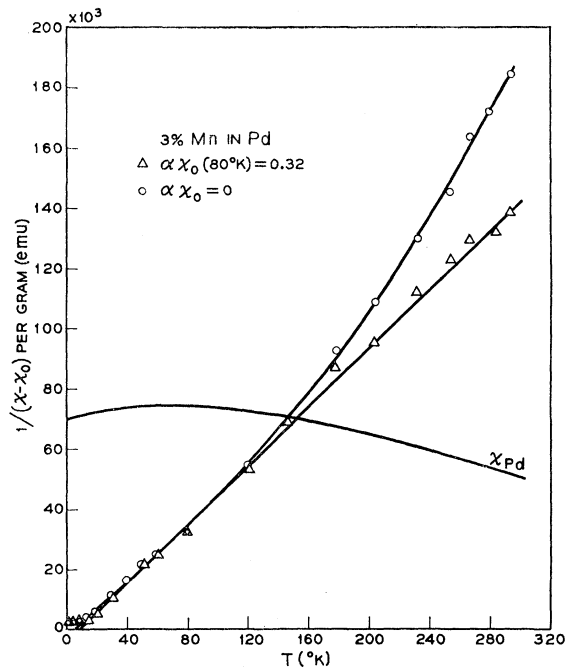


FIG. 11. $1/\chi-\chi_0$ curves of 3% Mn in Pd with and without enhancement correction; χ_{Pd} in arbitrary units.

intersection of the $1/\chi$ curve with the temperature axis was 45°K compares well with the value of 40°K obtained from the H/σ versus σ^2 method.²¹ The number of Bohr magnetons per Ni atom derived from the slope of the $1/\chi$ curve for this concentration was 7 ± 0.3 . The plot of $1/(\chi-\chi_0)$ for 3% Mn in Pd is shown in Fig. 11. As in the case of Fe and Co, a bend is observed in the curve around 120°K where the Pd susceptibility begins to change appreciably. We expect here also some enhancement of the Mn localized moment. Using the same procedure as before, Eq. (7), we have chosen the value for α so as to get a linear $1/(\chi-\chi_0)$ dependence as shown in the lower curve of

²¹ H/σ versus σ^2 method. J. S. Kouvel, G. D. Crane, Jr., and J. J. Baker, J. Appl. Phys. 29, 3, 518 (1958).

Fig. 11. From it we obtain the effective moment at 80°K to be $6.3 \mu_B$. The enhancement factor at this temperature is 35%. The unenhancement effective moment is $4.59 \mu_B$ compared with the effective moment of $4.79 \mu_B$ derived by Gerstenberg from high-temperature measurements. The Curie temperature derived from the slope is 8°K, close to the value of 9°K derived by the H/σ over σ^2 method. The Curie temperature derived from high-temperature extrapolation is +60°K²⁰ and is unrealistic.

b. EPR of Gd in Pd with Iron-Group Ions in Dilute Solution

1. *Ni-doped Pd alloys.* The g values and linewidths of 3% Gd in Ni-doped Pd alloys at 47.7 kMc/sec for various temperatures are given in Table III. Figure 12

TABLE III. g value of 3% Gd in Pd with Ni impurities.

Ni concentration (mole %)	Temperature (°K)	g value	Linewidth of 10% (G)
none	20.4	1.888 ± 7	650
none	4.2	1.927 ± 7	1000
none	1.6	1.931 ± 7	1060
0.2	20.4	1.862 ± 7	840
0.2	4.2	1.897 ± 7	1070
0.2	1.6	1.924 ± 7	1300
1	20.4	1.860 ± 10	1160
1.5	20.4	1.830 ± 10	1400
1.5	4.2	1.897 ± 10	1400
1.5	1.6	1.895 ± 10	1200

shows that the absolute value of the g shift at 20°K increases with the increase of the Ni concentration up to about 1.5% Ni. The increase of shift is followed by an

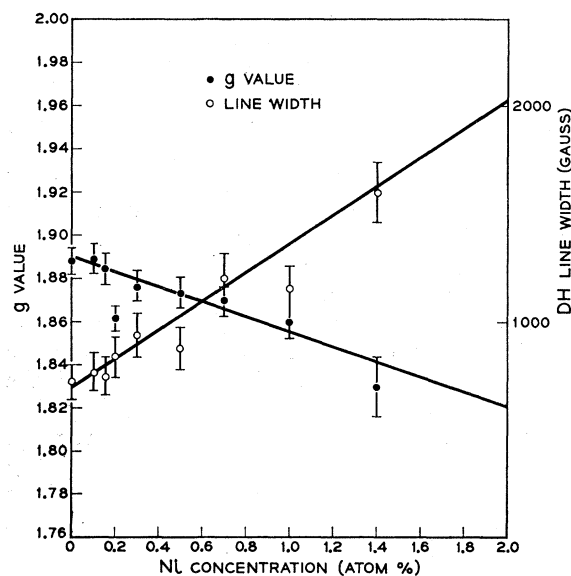


Fig. 12. g value and line width at 20°K of 3% Gd in dilute Pd-Ni alloys as a function of the Ni concentration.

increase of linewidth (Fig. 12). At 2% Ni and 20.4°K the linewidth was too broad and therefore too weak to obtain any measurable data. The increase of the absolute value of the g shift is probably due to the increase of the density of states as indicated in the susceptibility measurements. No Ni ferromagnetic resonance was observed for a Pd_{0.965}Ni_{0.035} alloys down to 1.6°K.

2. *Fe- and Co-doped Pd alloys.* As mentioned in the preceding section, both Fe and Co become ferromagnetic with high Curie temperature at very low concentration. This has restricted our investigation of the effect of these elements on the Gd resonance in Pd in the paramagnetic state to concentrations below 0.3% at 20°K. Above 0.3% the alloys become ferromagnetic at 20°K, washing out the Gd resonance. For 0.4% iron, a ferromagnetic resonance is observed at $g \sim 2.20$ with or without the presence of the Gd. No resonance was observed for the case of 0.5% Co in Pd without Gd although we searched down to 1.6°K. At low concentrations we had difficulties in the determination of the iron and cobalt concentration in our samples.

The g values and linewidths of 3% Gd as a function of the Fe and Co concentration and the temperature are given in Table IV. For 0.1% Co two opposite

TABLE IV. g value of 3% Gd in Pd with Fe and Co impurities.

Impurity concentration (mole %)	Temperature (°K)	g value	Linewidth $\pm 10\%$ (G)
0.1 Fe	20.4	1.89 ± 0.01	1000
0.1 Fe	4.2	1.92 ± 0.01	890
0.1 Fe	1.6	1.984 ± 0.007	980
0.2 Fe	20.4	1.906 ± 0.007	950
0.2 Fe	4.2	1.96 ± 0.01	920
0.3 Fe	20.4	2.00 ± 0.01	2800
0.1 Co	20.4	1.847 ± 0.007	600
0.1 Co	4.2	1.975 ± 0.007	990
0.1 Co	1.6	1.982 ± 0.007	1290
0.2 Co	20.4	1.89 ± 0.01	810
0.3 Co	20.4		~ 2000
none	20.4	1.888 ± 0.007	650
none	4.2	1.927 ± 0.007	1000
none	1.6	1.931 ± 0.007	1060

effects are observed, (1) a decrease at 20.4°K of the Gd g value with respect to the Gd g value of the Co-free alloy, (2) an increase of the Gd g value with decreasing temperatures. We associate the first effect with the increase of the Pauli susceptibility of the metal similar to what we have observed in the Ni-doped Gd-Pd alloys. The second effect which is temperature-dependent is associated with the polarization of the conduction electrons by the localized moments of the Co ions. From the slope of the additional Gd g shift with temperature we obtain a negative sign for the exchange interaction between the Co localized moment and the conduction electrons. In the case of iron the

results are not as conclusive as in the case of Co. At 20°K we observe for 0.3% Fe a very broad line (2800 G half-width) shifted towards $g=2.00$, but the line was very intense, so that we believe it to be a ferromagnetic resonance line. However, from the shift of the 0.1% Fe line with temperature and the slight increase of g value with concentration up to 0.2% Fe we may conclude that the sign of the Fe conduction-electron interaction is negative.

3. Mn-doped Pd alloys. Unlike the other transition element ions, Mn has shown an EPR line in metallic solutions. 2% Mn in Pd gives a broad line of 1500 G with a positive shift $\Delta g = +0.08$, ($g = 2.08$), indicating a positive exchange interaction with the valence electrons. This resonance will be discussed elsewhere.²² The effect of 2% Mn on the EPR of 2% Gd in Pd at 20°K was a slight shift of the Gd line: $Gd = 1.903 \pm 0.007$, $DH = 1200 + 100$. The Mn line was not observed in this alloy. Since the conduction electrons relax towards the spontaneous magnetization of the localized moment and since the g values of both Gd and Mn are close one should not expect a large effect of one on the other as far as g shifts are concerned.⁸ However, Mn broadens the Gd line considerably (from 650 to 1200 G). Probably, the Gd does the same to the Mn line, and this can be the reason for not observing the Mn line.

C. Pd-Uranium System

a. Susceptibility

The U-Pd system forms a solid solution up to 20 at. % U. Above 20% U mixed phases with the UPd₃

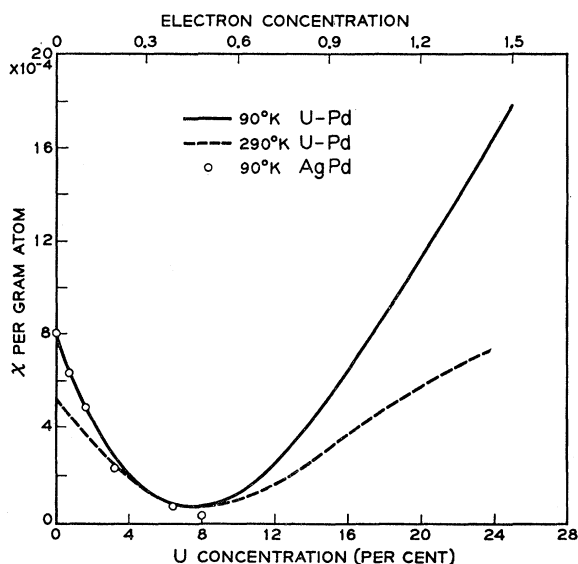


FIG. 13. Susceptibility of PdU alloys as a function of U concentration, and electron concentration at 290 and 90°K after Bates and Leach (Ref. 12); susceptibility of Pd-Ag alloys as a function of electron concentration. See Ref. 12.

²² D. Shaltiel and H. J. Wernick (to be published).

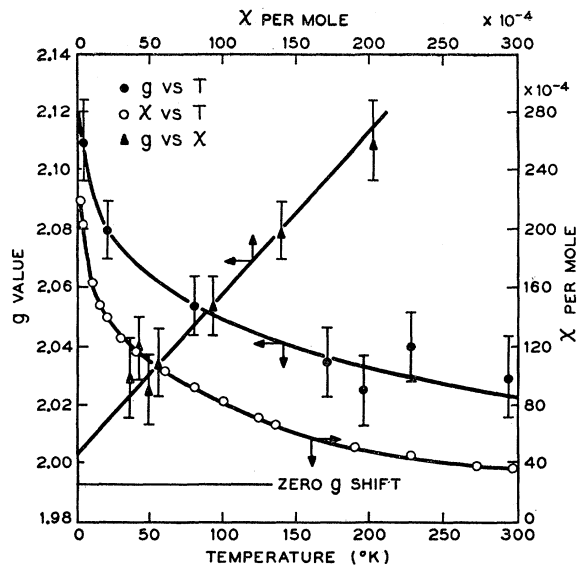


FIG. 14. g value of 2 at. % Gd in UPd₃ as a function of temperature. Susceptibility of Gd-free UPd₃ as a function of temperature. Gd g value as a function of susceptibility obtained from above curves. Both parameters are an explicit function of the temperature.

intermetallic compound are obtained.²³ The susceptibility of the system UPd was measured by Bates and Leach¹² between 90 and 293°K, for uranium concentrations up to 30%. Their susceptibility at 90°K as a function of the uranium concentration is given in Fig. 13. These authors explained the initial decrease of the susceptibility by assuming that the uranium electrons enter into the almost full Pd d band. By plotting the susceptibility against electron concentration, they found that their curve coincides up to 9% U at 90 and 290°K with the normalized susceptibility curve for Pd alloys described in Sec. A.a if one assumes that six electrons per U atom enter into the d band (Fig. 13). The increase of the U susceptibility above 10% is believed to be due to the formation of a new band by the 5f electrons of the U atoms. Bates *et al.* assumed a Curie law and derived from a T versus $1/\chi$ plot a moment of 3.14 magnetons per U atom for U concentrations higher than 15%. From this moment they concluded that U is in the quadrivalent state. However, they did not take into account the temperature-independent part derived from a plot of χ against $1/T$ by extrapolating to $1/T=0$. This correction decreases the magnetic moment of UPd₃ to 2.10. We have measured the susceptibility of UPd₃ from 1.4 to 300°K (Fig. 14). Our results are slightly higher in the temperature range where our measurements coincide. The plot of $1/\chi$ versus T deviates from a Curie law below 90° even after subtracting the so-called temperature independent part. At 1.2°K, high field-saturation measurements

²³ H. B. Pearson, *A Handbook of Lattice Spacing and Structure of Metals and Alloys* (Pergamon Press, Inc., New York, 1958).

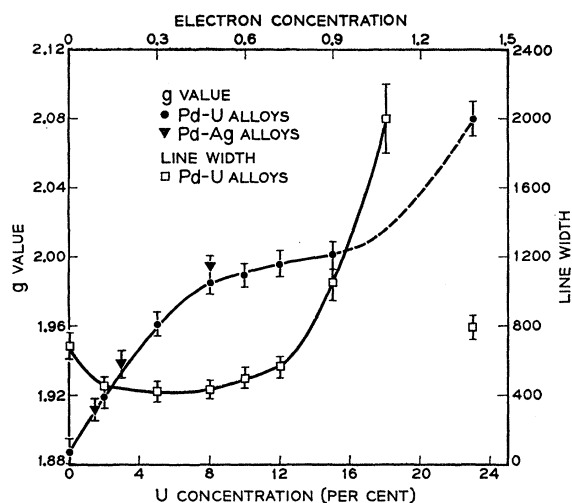


FIG. 15. g value and linewidth of 2 at. % Gd in Pd-U alloys as a function of U concentration and electron concentration; g value of 3 at. % Gd in Pd-Ag alloys as a function of electron concentration (see Ref. 1).

extrapolated to infinite fields show a moment of less than 0.06 Bohr magnetons per U atom in UPd_3 . EPR measurements discussed below show magnetic ordering at temperatures close to 4°K. We may therefore conclude that the simplified Curie picture does not hold in this case and one has to treat the problem more completely.

b. EPR of Gd in U-Pd Alloys

The EPR results of two mole % Gd in Pd-U alloys are shown in Fig. 15. We observe that the absolute value of the g shift $|\Delta g|$ decreases with the increase of the U concentration in the same way as the susceptibilities discussed before and that the initial g shift induced by the Pd metal almost goes to zero at about 9% U, that is, at the same U concentration where the Pd-U susceptibility is at its minimum. This correlation between the g shift and susceptibility is analogous to the one observed in the Pd-Ag alloys. Figure 15 shows that the g values of Gd in Pd-Ag alloys coincide within the experimental error with those of Pd-U if both are plotted on the same electron concentration scale, in analogy to the behavior of the susceptibility of the two alloy systems (Fig. 13). This supports our previous assumption that the g shift is due to the interaction of the localized moment with the d -band electrons and that this interaction is determined by the general band properties of the alloys.

For short-range polarization of the conduction electrons around the U atoms, we would expect an increase of the linewidth with the increase of the concentration due to the random distribution of the U ions, the contribution to the linewidth being roughly proportional to slope of the g value against concentration. Instead, we

observe a decrease of the linewidth up to 3% U where the linewidth levels off, Fig. 15.

A small increase of the Gd g value is observed from 9 to 15% U. A sharp increase of the linewidth is observed around 11%. This increase of the linewidth has prevented an accurate determination of the g value between 15 to 20% U. At higher U concentrations, the alloys contained the UPd_3 phase,²³ and hence, we studied only the alloys with less than 20% U, and the compound UPd_3 . In this compound, Gd showed temperature-dependent positive g shifts (Fig. 14). These shifts are a linear function of the susceptibility of pure UPd_3 as shown in Fig. 14, where both shift and susceptibility are an explicit function of the temperature. Extrapolation to zero susceptibility gives a g value of 2.00 close to the value for the free Gd ions. The linewidth at 20°K in the ordered compound UPd_3 is smaller than the linewidth in the unordered alloy. An increase of the linewidth is observed at temperatures below 20°K for UPd_3 (Fig. 16). At 1.6°K the line is very broad. The estimated half linewidth is about 6000 G. This broadening indicates that at these low temperatures some magnetic ordering is taking place. A similar increase in linewidth was observed for Gd in Pd at very low temperatures¹ where this increase was attributed to the ordering of the Gd, though the linewidth was not as large (2000-G half-width at 1.4°K). It is possible that the increase of the linewidth in the UPd_3 case is due to some magnetic ordering which occurs also in the undoped system, e.g., among the $5f$ electrons of the uranium.

D. UNi_5 and CaCu_5 Systems

a. Susceptibility Measurements

The UNi_5 and CaCu_5 structures are cubic and hexagonal, respectively.²⁴ The UNi_5 is closely related to the MgCu_2 cubic laves phase and the CaCu_5 is related to the MgZn_2 hexagonal laves phase. There are seven known compounds having the UNi_5 structure and 24 known compounds having the CaCu_5 structure.²⁵ The list of the AB_5 compounds investigated is given in Table V. The B elements are Ni, Ir, Pt, and Cu characterized by having an almost full or a full d shell. The A elements are Y, La, Th, and U. These compounds are suitable for EPR investigation of Gd as the Gd goes substitutionally into the A sites.

Nesbitt *et al.*²⁶ have observed very low susceptibilities for LaNi_5 and YNi_5 compounds and concluded that the Ni atoms do not carry any moment. We have repeated their measurements in order to obtain a more accurate value for the Pauli susceptibility of these

²⁴ A. E. Dwight, Trans. ASM 53, 379 (1961).

²⁵ *Electronic Structure and Alloy Chemistry of the Transition Elements*, edited by P. E. Beck (Interscience Publishers, Inc., New York, 1963).

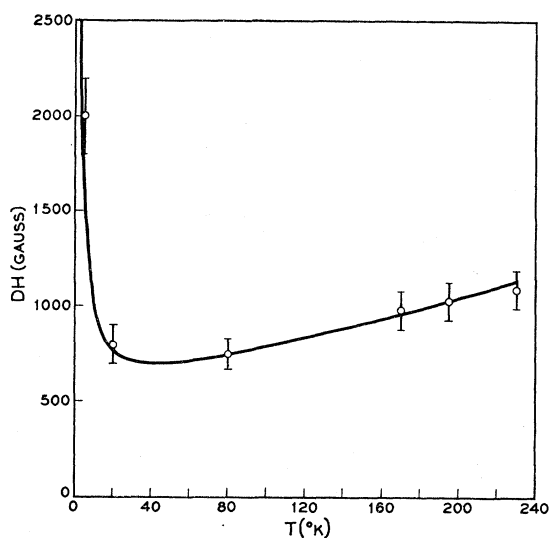
²⁶ E. A. Nesbitt, H. J. Williams, J. H. Wernick, and R. C. Sherwood, J. Appl. Phys. 33, 1674 (1962).

TABLE V. EPR of 5 mole % of Gd substituted in the A site in AB_7 compounds at 20°K at 47.7 kMc/sec.

Compound	Structure	g value	Linewidth (G \pm 10%)	g shift $g-g_s$
LaNi ₅	CaCu ₅	1.877 \pm 0.007	550	-0.12
YNi ₅	CaCu ₅	1.900 \pm 0.007	525	-0.10
ThNi ₅	CaCu ₅	1.913 \pm 0.007	525	-0.09
UNi ₅	UNi ₅	1.953 \pm 0.007	470	-0.05
ThIr ₅	CaCu ₅	1.973 \pm 0.007	640	-0.03
YCu ₅	CaCu ₅	2.000 \pm 0.007	350	00
LaPt ₅	CaCu ₅	2.022 \pm 0.010	860	+0.02
GdNi ₅ ^a	CaCu ₅	1.942 \pm 0.007	905	-0.06
GdCu ₅ ^b	CaCu ₅	2.009 \pm 0.007	875	+0.01

^a 78°K.
^b 65°K.

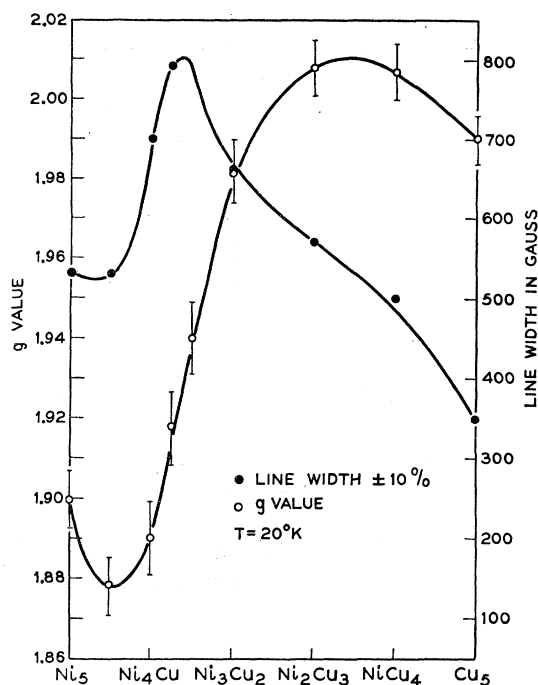
compounds. Our measurements have confirmed the low susceptibility of these compounds though a very small ferromagnetic moment was measured even at room temperature. We attribute the ferromagnetism to aggregates of Ni atoms due to slight deviations from the stoichiometric composition. This effect interfered with the detailed determination of the susceptibility as a function of temperature. However, from the slope

FIG. 16. Half-width at half intensity of 2 at. % Gd on UPd₃ as a function of the temperature.

of the magnetic moment against the magnetic field at high field, measured at 1.4 and at 300°K we estimate the Pauli susceptibility to be about 10^{-3} emu per mole. This value is two times larger than the molar Pd susceptibility at the same temperature, and comparable to the molar susceptibility of the alloy Pd_{0.95}Rh_{0.05}.

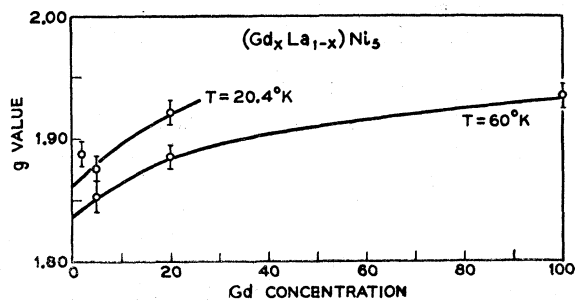
b. EPR Measurements

We have investigated the EPR of Gd substituted in the A site of the AB_5 compounds as a function of temperature and Gd concentration. Table V gives the g values and the linewidths of 5 mole % of Gd at 20.2°K in these compounds. Except for LaPt₅ all compounds with an unfilled d -shell element in the B

FIG. 17. The g value and linewidth of 5 mole % Gd in $YNi_xCu_{(5-x)}$ as function of Ni-Cu concentration at 20.4°K.

site, having a negative g shift. The largest negative g shifts are observed for the compounds containing Ni. Their magnitude decreases with the increase of the valence of the A-site atom, this valence being three for La and Y, four for Th and six for U. As negligible g shifts are observed for Cu₅ compounds, we were interested to find out how the g shift of Gd changes in the alloys $YNi_xCu_{(5-x)}$. We observed (Fig. 17) that the g value has a minimum at the composition $YNi_{4.5}Cu_{0.5}$ and that the g shift is small for large Cu concentrations. The Gd g value in $Gd_xLa_{1-x}Ni_5$ in the paramagnetic state increases as a function of the Gd concentration (Fig. 18). A decrease of the g value is also observed with temperature from 20 to 60°K (Fig. 18).

Additional Gd g shifts were obtained when the atoms at the A sites of the AB_5 compounds were

FIG. 18. The g value of Gd in $(Gd_xLa_{1-x})Ni_5$ as function of the Gd concentration at 20.4 and 60°K.

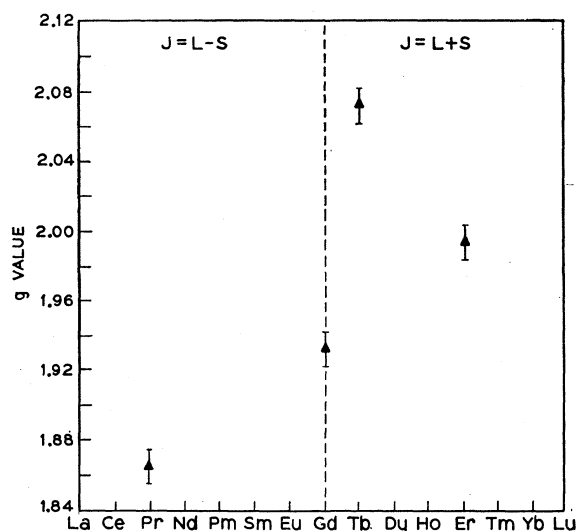


FIG. 19. The g value of 20 mole % Gd in YNi_5 doped with some RE elements at 20.4°K (10 mole % for Tb and Er, 20 mole % for Pr). The RE and Gd were substituted in the Y site.

partially substituted by the RE ions Pr, Tb, and Er (Fig. 19). The effect of Tb and Er, whose positions in the periodic table are to the right of Gd, was to increase the g value, while the effect of Pr, whose position is to the left of Gd, was to decrease the g value, in analogy to our observations in the Pd alloys.

IV. DISCUSSION

A. Line Shift

The experiments of the previous section show that the line-shift phenomena are satisfactorily to be described by an effective exchange interaction $JS \cdot s$, and expressions (5). J is found to be negative for Gd in Pd and its alloys, and in $LaNi_5$ and YNi_5 .

A close analogy between the cases of Pd and $LaNi_5$ is brought out in Fig. 20, where the dependence of the g values on the valence-electron concentration is compared. This concentration was varied by alloying Pd with Rh and with Ag, and by alloying Ni_5La with Cu_5La . In the periodic system Rh and Ag are neighbors of Pd, and Cu stands next to Ni. All three substitutions are assumed to change the valence-electron concentration by one, and for partial substitutions the concentrations are linearly interpolated. The concentration scales for the Pd alloys and the $LaNi_5$ alloys are shifted so as to bring the minimum Gd g values to coincidence. Under these conditions, we find that in both alloy series the g values in function of valence-electron concentration are nearly identical.

The better known of the two alloy series compared here is the Rh-Pd-Ag series. The susceptibility has in this case a sharp maximum for Pd, and falls to a very low value for a change in the effective electron con-

centration of $+0.6$. This well-known effect²⁷ has given rise to the notion that in Pd, the d band contains 0.6 holes per atom, and that these holes are being filled in as the valence-electron concentration is increased.

An analogous effect is observed in Ni. The saturation magnetization of Ni is 0.6μ Bohr per atom, and decreases linearly with valence-electron concentration, reaching zero at the composition $Ni_{0.4}Cu_{0.6}$.

We may then assume that both in Ni and in Pd, 0.6 d holes per atom are present, and that these holes can be filled up in the manner discussed. The analogy in the two cases is related to the identity of their crystal structures, and to their position in the same column in the periodic system. The fact that Ni is ferromagnetic and Pd only highly paramagnetic may be related to the fact that the density of atoms is 1.4 times higher in Ni than in Pd. In $LaNi_5$, the density of the Ni atoms is reduced, and hence the exchange interaction left is, as in Pd, just large enough to produce the high paramagnetic susceptibility reported in Sec. III ($CaCu_5$ compounds).

The close analogy in the g shifts observed in Pd and $LaNi_5$ establishes the above relation between their magnetic properties in much more detail than the static susceptibility measurements which, in the case of $LaNi_5$, were difficult in view of the residual ferro-

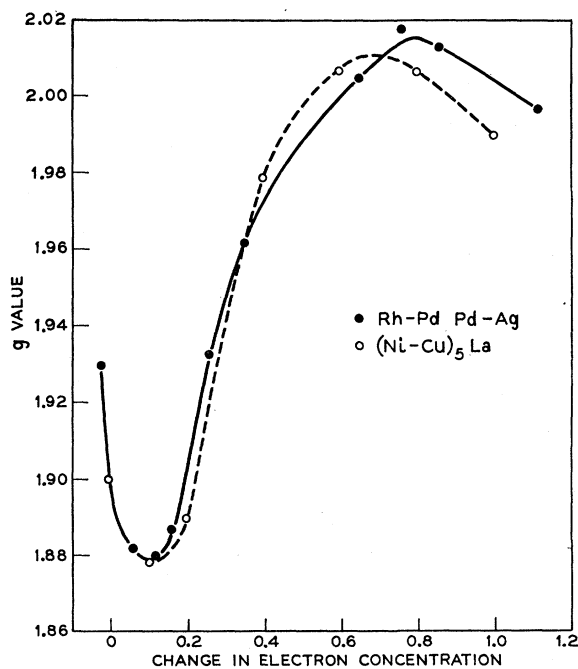


FIG. 20. Comparison of the Gd g values at 20.4°K in Rh-Pd Pd-Ag alloys¹ and Ni_5La Cu_5La mixed intermetallic compounds as a function of the change in the electron concentration. The two curves were shifted horizontally so that their two minima coincide. The zero in the electron concentration is arbitrary.

²⁷ N. F. Mott and H. Jones, *The Theory of the Properties of Metals and Alloys* (Dover Publications, Inc., New York, 1958).

magnetism due to stoichiometric fluctuations, Sec. III (CaCu₅ compounds). The fact that other rare earths produce similar additional shifts and widths further confirms our picture, as will be seen below.

It is understandable that the g shifts should decrease as the three valent atoms La and Y are replaced by Th and U which are of higher valency, since the additional valence electrons tend to diminish the number of d holes.

The shifts also diminish as Ni is replaced by Ir and Pt. These two atoms are the $5d$ analogs of the $3d$ atoms Co and Ni, and show only a weakly enhanced paramagnetism in the elemental state.

The strong parallelism between Pd, LaNi₅, and YNi₅ indicates that the effective exchange interaction between Gd and the magnetized $3d$ and $4d$ bands is *negative*. Similar negative exchange interactions were observed in almost full $4d$ and $5d$ bands in laves phase compounds.²⁸ This indicates that the origin of these interactions is not to be found only in the simple direct exchange interaction which was considered by the authors cited in Ref. 5 who were the first ones to treat the ion-conduction-polarization phenomena. This point was already discussed in our first paper.¹ Several authors (Anderson and Clogston,²⁹ Koidé and Peter³⁰) have discussed mechanisms that lead to negative polarization. The total effective exchange interaction is then the result of a balance of the positive and negative contributions, and in the case of the interaction between Gd and the d bands, we find experimentally that the negative interactions are the dominant ones. As the d holes are filled up, we find that the g shift becomes slightly positive (Fig. 17). This reversal of sign suggests that the effective exchange interaction is positive between the Gd ions and s electrons. The small magnitude of these positive shifts correlates with the low value of the s -electron susceptibility.

A much stronger positive g shift is found in the case of UPd₃. As the U concentration in the U-Pd system is increased towards 25%, we observe a change of the g value from $g=1.88$ to $g=2.08$. The g shift changes its sign from -0.12 for pure Pd to $+0.8$ at UPd₃. Gd may thus have either negative or positive interactions. In particular, we propose that the interaction between Gd and the d band in the Pd lattice is negative, and that the interaction between Gd and the $5f$ band which starts to be filled as the U concentration increases^{31,32} is positive.

The marked temperature dependence found for LaNi₅ (Fig. 18 shows a 20% increase between 20 and 60°K) may be interpreted as an indirect measurement

of the temperature dependence of the d -band susceptibility. A direct measurement of the static susceptibility in LaNi₅ is not possible, as was explained above. On the other hand, in Pd we have verified that the known dependence of the susceptibility between 20 and 80°K is indeed accompanied by a proportional change in the g shift.

Within the framework of the simple theory set forth in Sec. II, we expect no dependence of the Gd/ g shift on the Gd concentration, since the coupling between the Gd ions represents an effective exchange interaction. In the case of the Pd alloys, there was indeed no such dependence observed. However, in (Gd _{x} La _{$1-x$})Ni₅ we could experiment with much bigger Gd concentrations. Figure 18 shows that under these conditions a slight dependence of the g value on the Gd concentration is found. The slope of the g value versus concentration curve is more than one order of magnitude smaller than the slope for the other rare earths, and the curve is nonlinear. This concentration dependence is hardly a consequence of the change in the lattice parameters only since bigger changes of these parameters occur between LaNi₅ and YNi₅, whereas the difference in their g values is smaller. Instead, the effect may be due to saturation of the d -hole susceptibility due to the large polarization occurring at high concentration and to the interpenetration of the different polarization clouds around individual atoms.

Estimates of the values of the exchange interaction \bar{J}_a , defined in Sec. II, can be obtained from Eq. (5'). In this equation \bar{J}_a is related to quantities that can, in principle, be experimentally determined. χ_0 is the susceptibility of the valence electrons responsible for the shift.

In the case of Gd in Pd we assume $g_e=2$, and use $\chi_0=8.7 \cdot 10^{-4}$, $n_0=6.8 \cdot 10^{22}$. This leads to $\bar{J}(\text{Pd})=-0.009$ eV.

In the host metals Pd (Fig. 6) and YNi₅ (Fig. 19), we were able to measure the g shifts induced by the presence of other rare earths. The measurements are particularly complete in the case of Pd. Equation (5'') permitted us to evaluate \bar{J}_{RE} for this case and the results are given in Table II and in Fig. 21. The same

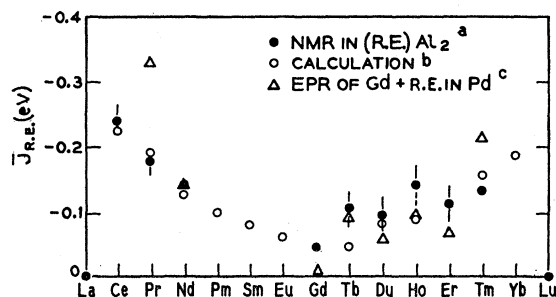


FIG. 21. \bar{J}_{RE} from the nuclear magnetic resonance measurement in (RE)Al₂ (see Ref. 30); EPR measurements of RE in Pd+2% Gd, [This paper; values for $\alpha=5$ (Ref. 8)], and the calculation of Koidé and Peter.

²⁸ D. Shaltiel, J. H. Wernick, and V. Jaccarino, J. Appl. Phys. 35, 978 (1964).

²⁹ P. W. Anderson and A. M. Clogston, Bull. Am. Phys. Soc. 2, 124 (1961).

³⁰ S. Koidé and M. Peter, Rev. Mod. Phys. 36, 160 (1964).

³¹ M. S. Friedel, Phys. Chem. Solids 1, 178 (1956).

³² A. C. Gossard, V. Jaccarino, and J. H. Wernick, Phys. Rev. 128, 1038 (1962).

figure shows also the nuclear-magnetic-resonance measurements of Jaccarino *et al.*³³ for \bar{J}_{RE} in (RE)Al₂ and the values calculated by Koidé and Peter,³⁰ which are plotted on a different scale. The scale of these results depends on an accurate knowledge of the band parameters which is not yet available. It is, however, interesting and encouraging to notice that the dependence of the values for \bar{J}_{RE} of atomic numbers show a common trend for the three sets of values. The results given in Sec. III (iron-group elements in Pd) give indications on the effective exchange interaction between the valence electrons of Pd and the transition metal ions Fe, Co, Ni. The magnetic behavior of these ions in solution in Pd is much more complex than that of the rare earths, as these ions show moments which are much bigger than the ionic moments, and contribute also to the temperature-independent (host metal) susceptibility. We find a positive \bar{J} for Ni, and negative values of \bar{J} for Fe and Co. These findings may be compared with the determination of the fields seen by Sn nuclei in dilute solution in the metals Ni, Fe, and Co. These fields are again found to be positive in Ni, negative in Fe and Co.³⁴ The measurements, made by observation of the Mössbauer effect are, however, mainly sensitive to the polarization of the *s* electrons and the correlation with our results is therefore not clear. As discussed in Sec. III. B.c., the observation of the Gd resonance in Pd with Mn and Gd gave inconclusive results, presumably because of the closeness of the *g* factors of the Gd and Mn ions. The exchange interaction of Mn in Pd has, however, been measured more directly by the observation of the Mn EPR itself, which will be discussed elsewhere.²²

In the case of Gd in UPd₃, we can deduce the value of $\Delta g_0/\Delta\chi_0$ directly from Fig. 14 and find it to be $\Delta g_0/(\Delta\chi_0 \text{ mole}) \sim 5$. This leads to $\bar{J}_{Gd}(\text{Pd}_3\text{U}) = +1.75 \times 10^{-4}$ eV.

Finally, in the case of GdAl₂ we do not know χ_0 . If we use, however, a calculated value for the free Pauli paramagnetism, based arbitrarily on $E_F = 5$ eV and 3 valence electrons per Gd atom, we obtain for³⁵ $\Delta g_0 = -0.01$ the value $\bar{J}_{Gd}(\text{GdAl}_2) = -2.2 \times 10^{-2}$ eV.

In all cases we obtain values for \bar{J}_a which are considerably smaller than the corresponding values which can be deduced from the atomic spectrum of Gd. Since the occurrence of both signs tells us that \bar{J}_{Gd} is the result of positive and negative contributions, this is not surprising.

B. Linewidths

In our earlier paper (Fig. 4 of Ref. 1) we noted that the linewidth increases parallel to the *g* shift. A similar correlation appears in Table V, where the linewidths

and *g* shifts are listed for the compounds of the CaCu₅ structure, and for UNi₅. For example, the linewidth of Gd in YCu₅ with no shift, is 350 G, whereas in YNi₅ where the *g* shift is -0.10 , the linewidth is 550 G. We would expect such a correlation through a relaxation process analogous to the Korringa process. However, as noted before¹ the observed broadenings are only a small fraction of the ones expected from Korringa's relation. Also, in ThIr₃ and LaPt₅, the linewidths are larger in spite of the small *g* shifts of these compounds.

It becomes clear that the Korringa process is not fully operative, and that other broadening mechanisms are also important.

An interesting example of another type of broadening appears in the mixed (Ni_xCu_{1-x})₅Y compounds. The widths and *g* shifts in these compounds are shown in Fig. 17. Superimposed on the decrease of the linewidth in Cu₅Y versus the linewidth in Ni₅Y mentioned above, there is a significant contribution to the linewidth which is large where the derivative of the *g* shift versus concentration is large. A natural explanation of this contribution is that it is due to local fluctuations in the Ni concentration of the alloy. The scale on which these fluctuations occur must be larger than the range of the exchange interaction between Gd ions and conduction electrons, otherwise the fluctuations would be averaged out. We will see below that this range amounts to several lattice distances to that we obtain a nontrivial lower limit for the scale of the fluctuations.

We find thus that the study of the Gd resonance in alloys can be a useful tool for the study of the microstructure in these alloys. For instance, the relatively narrow lines observed for Gd in Pd indicate that Gd was indeed dissolved in Pd, in spite of the large difference in the atomic radii of Gd and Pd. On the other hand, we have not been able to dissolve La in Pd. Instead, as we have seen in Sec. III (rare earth in Pd) addition of La to Pd caused a second resonance line to appear in the Gd spectrum. This second line gives a clear indication of the formation of a second phase even though in the x-ray spectrum, this second phase manifested itself only in a broadening of the diffraction lines.

The study of the influence of other dilute rare earths on the linewidth of the Gd resonance line leads to an interesting conclusion about the range of the conduction-electron polarization. The correlation between broadening *B*, shift *S*, and range appears in a particularly simple way if we choose for the interaction function the simple model function $f_M(\mathbf{x})$ introduced in Sec. II. The parameter $R_M = S^2/B$ is, in this case, just equal to the fraction of the B atoms which reside within a sphere of radius r_0 . As we have observed values of $R_{\text{obs}} = (S/\Delta DH)^2$ as high as 5 (Table II), we obtain values for the range r_0 of the order of 10 Å. This estimate of the range can serve as a lower limit of the

³³ V. Jaccarino, B. T. Matthias, M. Peter, H. Suhl, and J. H. Wernick, *Phys. Rev. Letters* **5**, 251 (1960).

³⁴ A. J. F. Boyle, D. St. P. Bunbury, and C. Edwards, *Phys. Rev. Letters*, **5**, 553 (1960).

³⁵ M. Peter, *J. Appl. Phys.* **32**, 338S (1961).

scale of the fluctuations of the Ni concentration in $(\text{Ni}_x\text{Cu}_{1-x})_5\text{Y}$ discussed above. The observed value $S^2/B = R_{\text{obs}} = 5$ can also be compared with the values R_Y or R_K derived from the free-electron model.

For $c_B = 2 \times 10^{-2}$, $n/n_0 = 0.6$ we obtained $R_K \sim R_Y = 8.3 \times 10^{-3}$ in Sec. II.

It becomes clear that the effective range predicted by the free-electron model is one order of magnitude smaller than the range observed in the Pd alloys. An analogous long range of the valence-electron susceptibility was also observed in YNi_5 . This discrepancy between the observed effective range and the value predicted by the free-electron model has been discussed elsewhere.³⁶ Through the factor n/n_0 , R_Y and R_K depend on the diameter of the Fermi surface. In the free-electron model, this diameter is simply k_f . In the case of the almost full d band, the surface is likely to be no longer spherical. For instance, Fletcher³⁷ has proposed a Fermi surface consisting of thin cylinders, for the case of Ni. In such a case, the reciprocal diameter of these cylinders may determine the range of the d -hole polarization, and this range would be larger than R_Y . However, the discrepancy between R_{obs} and R_Y is so large as to make it likely that only a calculation which goes beyond the independent Bloch electron will explain the observed ranges satisfactorily.

ACKNOWLEDGMENTS

It is a pleasure to thank S. C. Abrahams, A. M. Clogston, S. Geschwind, A. C. Gossard, V. Jaccarino, J. M. Jauch, W. R. Scott, J. R. Schrieffer, L. R. Walker, and R. E. Watson for their helpful suggestions and discussions, Mrs. V. B. Compton for x-ray diffraction measurements in Pd alloys and D. Dorsi, J. B. Mock, R. C. Sherwood, and A. R. Stone for their technical assistance.

APPENDIX A: ALTERNATE DERIVATION OF Eq. (5')

The long-range nature of the valence-electron polarization discussed in Sec. IV. B, makes a description of the resonance of the ions of species A in terms of an exchange field possible. We write the Landau-Lifshitz³⁸

equations of motion of the magnetizations of the A system (\mathbf{M}_A) and of the valence electrons (\mathbf{M}_e).

These equations are

$$d\mathbf{M}_A/dt = \gamma_A \{ \mathbf{M}_A \times [\mathbf{H} + \lambda \mathbf{M}_e] \}, \quad (8a)$$

$$d\mathbf{M}_e/dt = \gamma_e \{ \mathbf{M}_e \times [\mathbf{H} + \lambda \mathbf{M}_A] \} - \alpha_e \{ \mathbf{M}_e [\mathbf{M}_e \times (\mathbf{H} + \lambda \mathbf{M}_A)] \}, \quad (8b)$$

with $\gamma_A = g_A \beta$, $\gamma_e = g_e \beta$, \mathbf{H} the applied d.e. magnetic field, and λ the molecular field constant.

λ is related to \bar{J}_A by $\lambda = \bar{J}_A / \beta^2 g_e g_A n_0$. g_e and g_A are the g values of the A systems and the valence electrons, respectively.

Now we consider the case where the relaxation rate of the valence electrons is much larger than the paramagnetic resonance frequencies. This limit may well apply to our experiments with d and $5f$ valence electrons in alloys and imperfect crystals. We have then to let the damping rate α_e go to infinity and obtain from (8b)

$$\mathbf{M}_A \times \lambda \mathbf{M}_e = \mathbf{M}_e \times H = \chi_0 (\mathbf{H} + \lambda \mathbf{M}_A) \times \mathbf{H}.$$

This relation inserted into (6a) gives

$$d\mathbf{M}_A/dt = \gamma_A (1 + \lambda \chi_0) \mathbf{M}_A \times \mathbf{H}.$$

From this we find immediately Eq. (5').

The result depends critically on the form of the Landau-Lifshitz relaxation term. Wangsness³⁹ has shown that this form of the relaxation term is, for thermodynamical reasons, the only admissible one. Equation (5') coincides also with one of the equations discussed by Hasegawa.⁴⁰ The other formula for Δg_0 discussed by Hasegawa derives from a relaxation term which is forbidden according to Wangsness and must therefore be discarded (see footnote 27 of Ref. 1).

We note that Eq. (5') is independent of χ_a . This means that the Gd ions which are coupled by an effective exchange interaction, will not shift their resonance frequency, in accord with a well-known theorem. On the other hand, this very theorem seems violated by the fact that the g shift Δg_0 still occurs even if $g_a = g_e$. The reason for this anomaly is of course that we assumed $\alpha_e \gg g_e \beta |\mathbf{H}|$, i.e., the valence electrons relax so fast that their resonance frequency is not observed.

³⁶ M. Peter, J. Phys. Radium **23**, 730 (1962).

³⁷ G. C. Fletcher, Proc. Phys. Soc. (London) **65**, 192 (1952).

³⁸ L. D. Landau and E. Lifshitz, Phys. Z.d. Soviet Union **8**, 153 (1953).

³⁹ R. K. Wangsness, Phys. Rev. **111**, 813 (1958).

⁴⁰ H. Hasegawa, Progr. Theoret. Phys. (Kyoto) **21**, 483 (1959).